Wavefront Sensing and Control Technology for Submillimeter and Far-Infrared Space Telescopes

Dave Redding
NASA / JPL

Abstract

The NGST wavefront sensing and control system will be developed to TRL6 over the next few years, including testing in a cryogenic vacuum environment with traceable hardware. Doing this in the far-infrared and submillimeter is probably easier, as some aspects of the problem scale with wavelength, and the telescope is likely to have a more stable environment; however, detectors may present small complications. Since this is a new system approach, it warrants a new look. For instance, a large space telescope based on the DART membrane mirror design requires a new actuation approach. Other mirror and actuation technologies may prove useful as well.

Acknowledgements

- NGST WFC Government Team:
  - At JPL: Scott Basinger, David Cohen, Phil Dumont, Joe Green, Andrew Lowman, Cathy Ohara, David Redding, Fang Shi, David Van Buren
  - At GSFC: Pierre Bely, Chuck Bowers, Laura Burns, Pam Davila, Bruce Dean, Peter Dogota, Kong Ha, Bill Hayden, Frank Liu, Gary Mosier, Peter Petrone, Gary Welter
- PSR, SMMM:
  - Eri Cohen, Ken Lau, David Redding, George Sevaston, Sam Sirlin
- SIM:
  - Mike Shao, Feng Zhao

Imaging and Wavefront Control

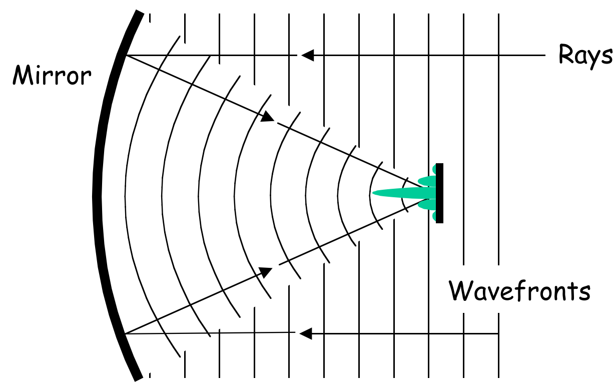

- A perfect optical system converts incoming wavefronts to concentric spherical wavefronts converging to a point image on a detector
- Imperfections arise from fabrication error, temperature changes, alignment shifts, strain relief, long-term dimensional change
  - Traditionally minimized using massive structures
- Wavefront control uses moving and deforming elements to compensate imperfections after launch
  - Replaces massive structures with computers and actuators

Principle of the wavefront control approach for NGST

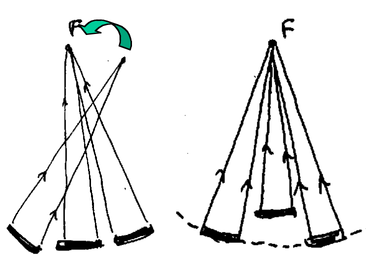

1. COALIGNMENT AND COFOCUSING

- Aligned to the accuracy of a single element telescope.
- Primary mirror piston ~ 5λ (10 microns) (limited by depth of focus of individual segment)

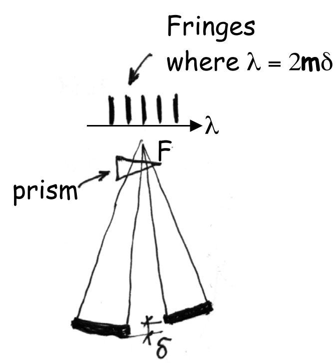

2. COARSE PHASING

Dispersed fringe sensing

WF error < λ

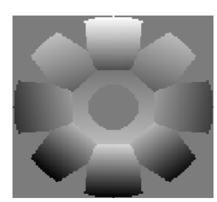

3. FINE PHASING

Phase retrieval

- WF measurement error < λ/100
- WF control error < λ/20

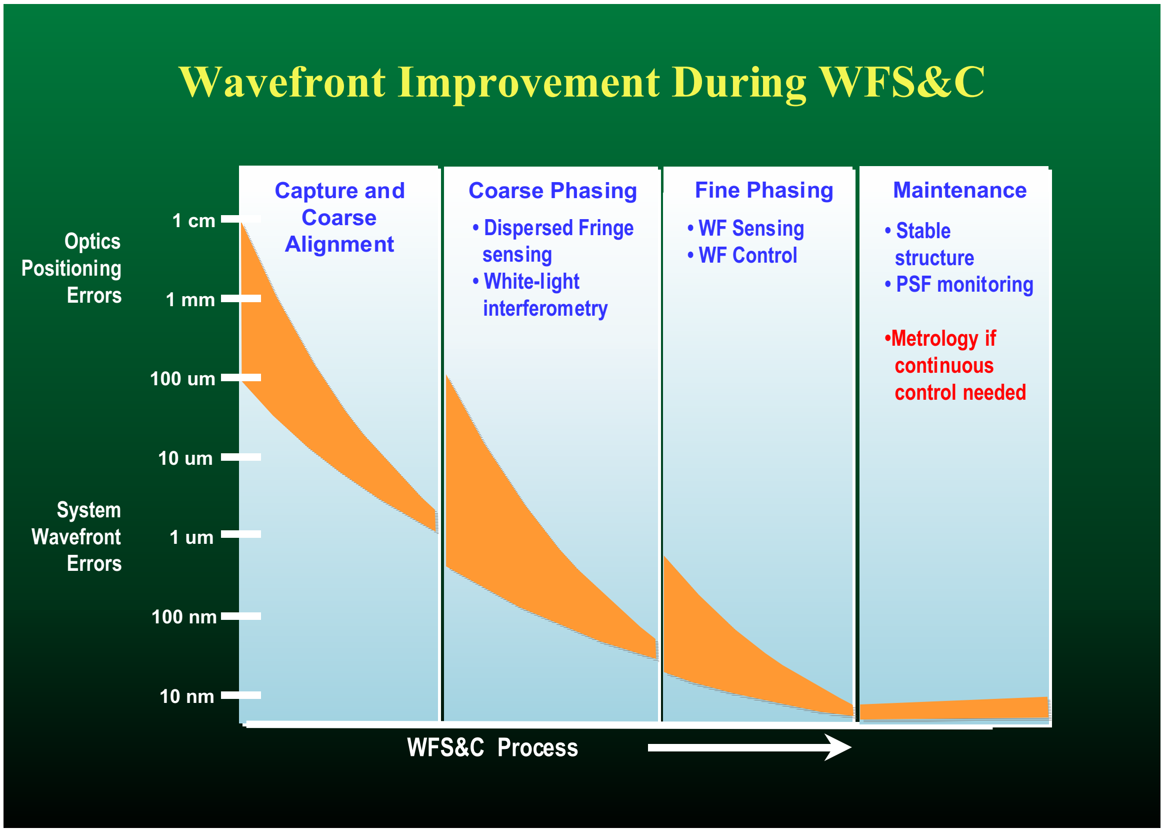

Coarse Phasing

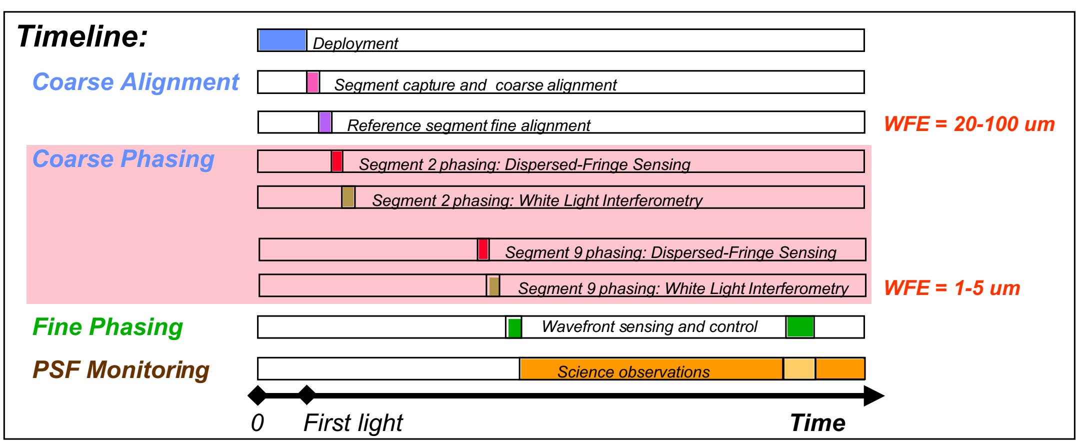

WCT-2 Testbed Layout

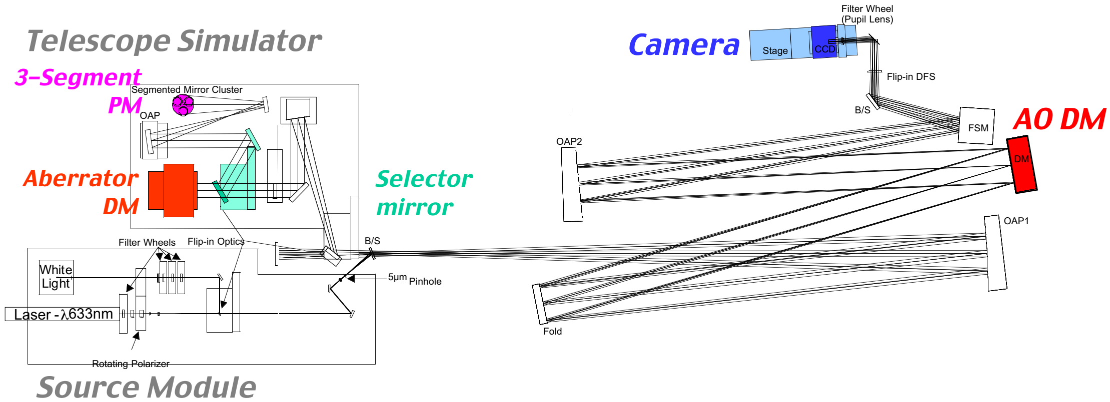

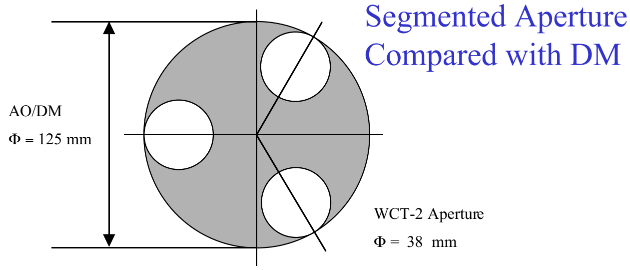

Dispersed Fringe Sensor (DFS)

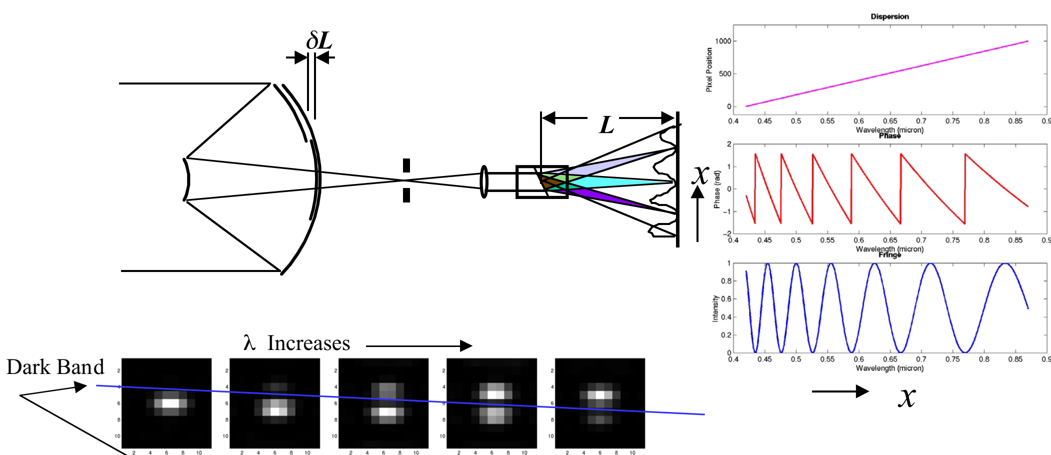

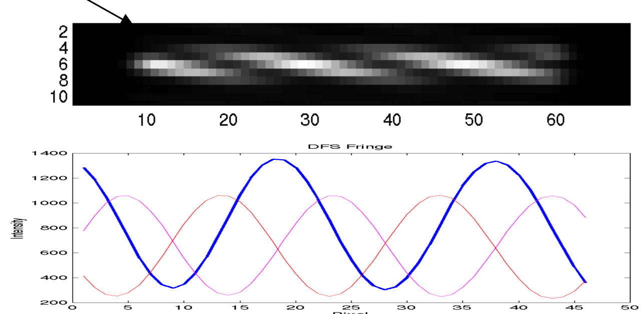

- DFS Modeled Fringe: DCATT Model
- Wavelength range: λ = 624.8 - 658.8 nm
- Piston error: δL = 7 µm

WCT-2 Demo: DFS Analysis (Segs #2 & #3)

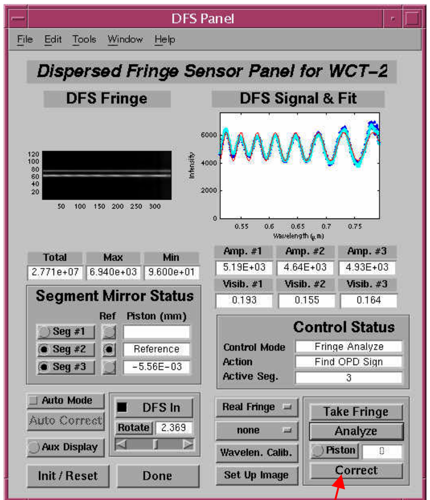

- Processed DFS image (Seg #1 tilted out)
- Processed DFS fringe from Seg #2 and #3 (dotted lines).
- DFS fitted curve (solid lines)
  - Fringe period determines piston magnitude
  - Relative phase between sidelobe traces determines the sign (up or down) of the piston
  - DFS analysis result:
    Relative Seg #3 Piston = -5.56 μm

Push here to implement piston correction

WCT-2 Demo: After Correction (Segs #2 & #3)

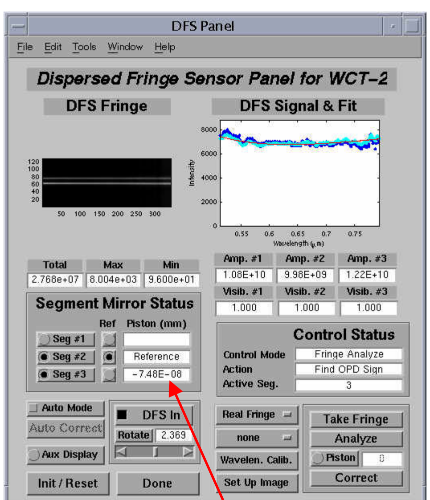

- Processed fringes after implementing correction show very little modulation
  - Modulation goes to 0 when segments are phased
  - Control has achieved sub-λ residual piston error

Detected piston reduced to near zero

White Light Interferometry (WLI) on WCT-2

- WLI scans one segment in piston, using relative to another segment or segments, while observing in broad-band light
- Peak occurs when segments are phased, secondary peaks occur as $\delta = 2n\lambda_{center}$
- Plots show the WLI signal and its fit before and after the correction of Seg #1 relative to Seg #3 (reference), while Seg #2 is tilted away
- Piston error before correction was $-0.68\ \mu m$
- After correction WLI detected $0.0\ \mu m$ piston
- Independent check using IPO measured 13 nm residual piston
- WLI detection error is dominated by 20 nm scan step size
- Other error sources include image under-sampling, lab seeing, and jitter

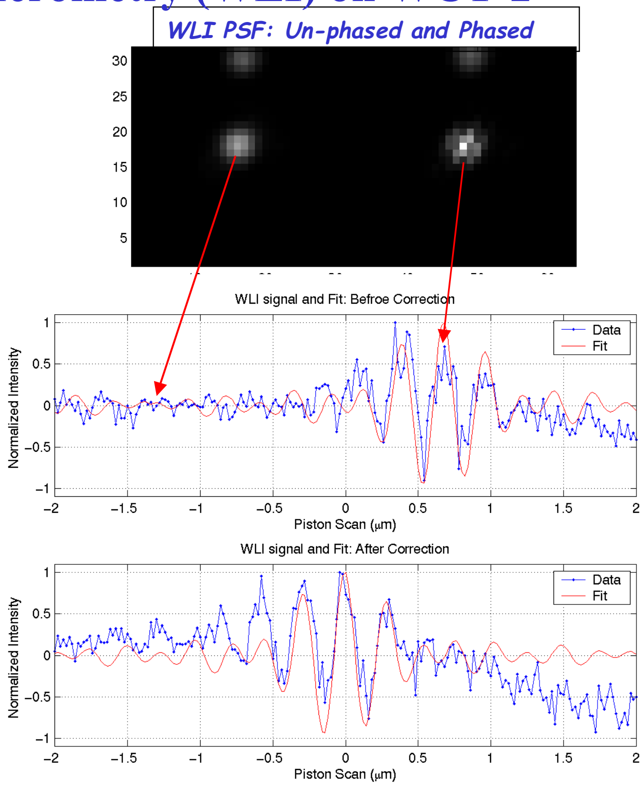

Coarse Alignment and Coarse Phasing Summary

- WCT-2 performance exceeds requirements and expectations
- Coarse alignment segment capture exceeds expected misalignments
  - Focusing algorithm -- camera stage test:
  - Before: > 10 mm (limited by camera FOV chosen)
  - After: < depth of focus (± 0.35 mm @ 633 nm)
- Segment mirror tilt errors:
  - Before: > 0.6 mrad (limited by segment actuator stroke)
  - After: < 4 μrad (limited by the jitter & seeing)
- Segment mirror piston errors:
  - Before: ~ 10 - 20 μm (limited by segment actuator stroke)
  - After: < 0.1 μm (DFS) (confirmed by PR and IPO)
    < 0.02 μm (WLI) (confirmed by PR and IPO)

Fine Phasing

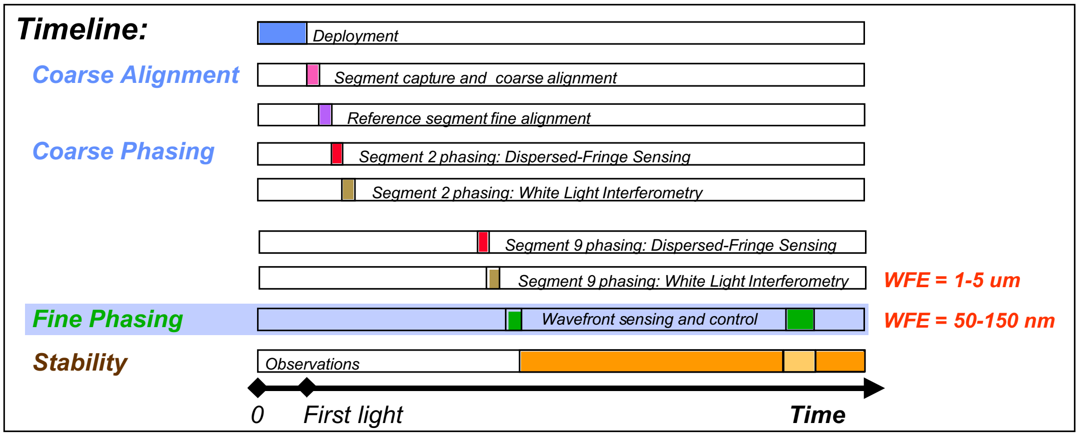

WF Sensing Using Images

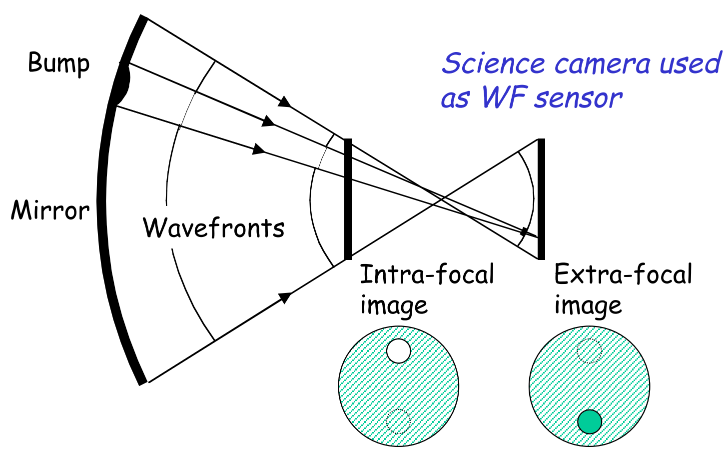

- A bump on the mirror surface shifts the focus of a patch of the beam
- This shows up as a bright spot on one side of focus and a dark spot on the other
- Computer processing of multiple defocussed images correlates the intensity variations in each, derives common WF phase map
- This phase map is then used to compute new control settings

Modified Gerchberg-Saxton Algorithm

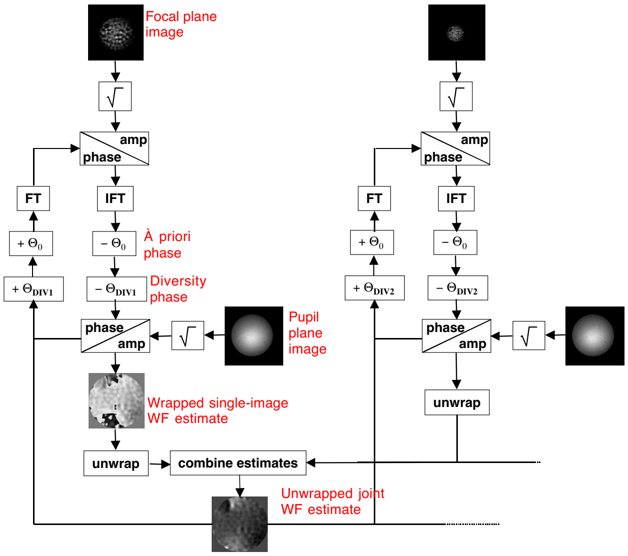

- Uses pupil image data to halve number of unknowns
- Uses defocussed images to improve visibility of aberrations
  - Reduces contrast between low, high-*f* effects
  - Reduces impact of jitter, other blurring
- Subtracts known phase (Θ_0, Θ_{DIV}) from the iteration to reduce iteration dynamic range

- Multiple images overdetermine solution to ensure uniqueness
  - Provides more data without introducing new unknowns
- Phase unwrapping allows estimation of WFE > λ
  - Joint unwrapping improves unwrapping robustness

Example from NGST WCT-1 Testbed

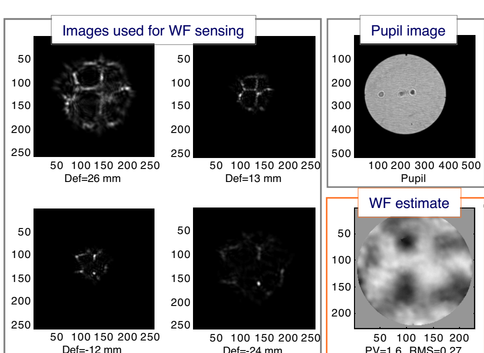

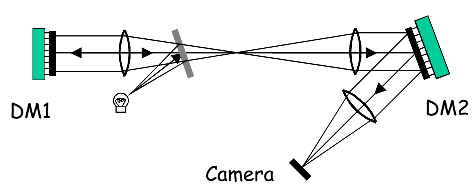

- Typical experiment: aberration applied using 1 DM...
  - Initial WFE = 1.6 waves peak-to-valley, 0.27 waves RMS

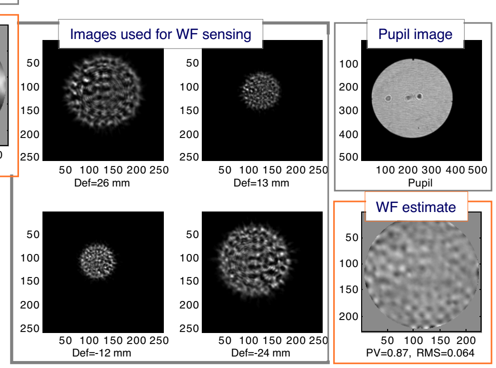

- ... and corrected using second DM
  - After control WFE = 0.87 waves PV, 0.064 waves RMS

Example from NGST WCT-2 Testbed

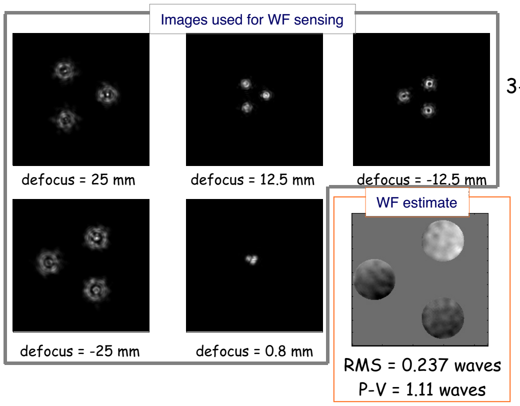

- Best results using WCT-2 require inclusion of at least 1 nearly in-focus image

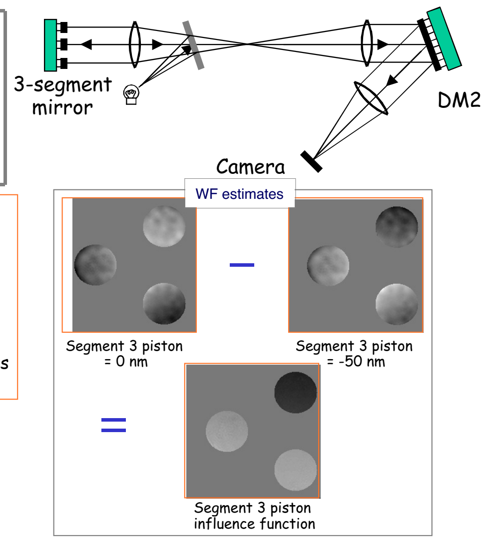

- Segment piston influence function determined by "poking" actuators and subtracting WFs

High Dynamic Range Retrieval & Control Examples

- WCT-1 Testbed Results
- High aberration injected at testbed SMDM
- Phase retrieved & unwrapped at 632.8 nm
- Phase controlled at testbed AODM

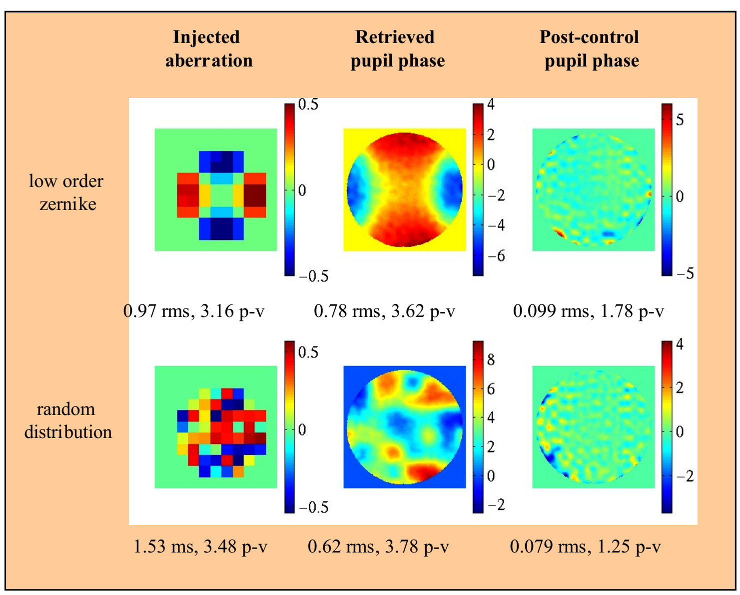

SIRTF Brutus Test

Telescope set up for vibe test

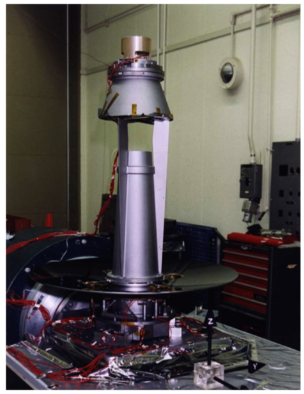

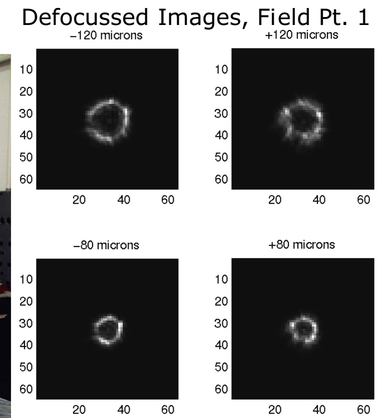

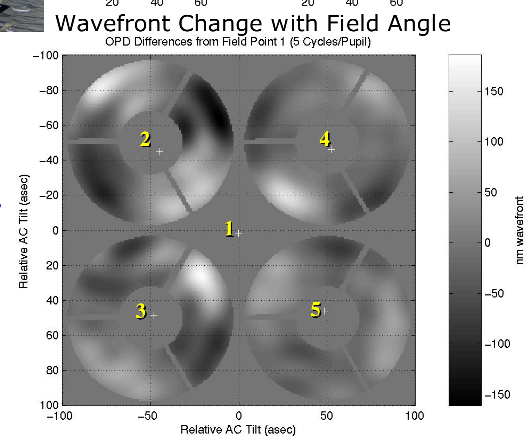

- SIRTF telescope end-to-end cryogenic optical test
  - Internal light source and autocollimating flat provide for in-chamber test capability
- Image-based WF sensing successfully measured WF at multiple field points

Mars Observer Camera Example

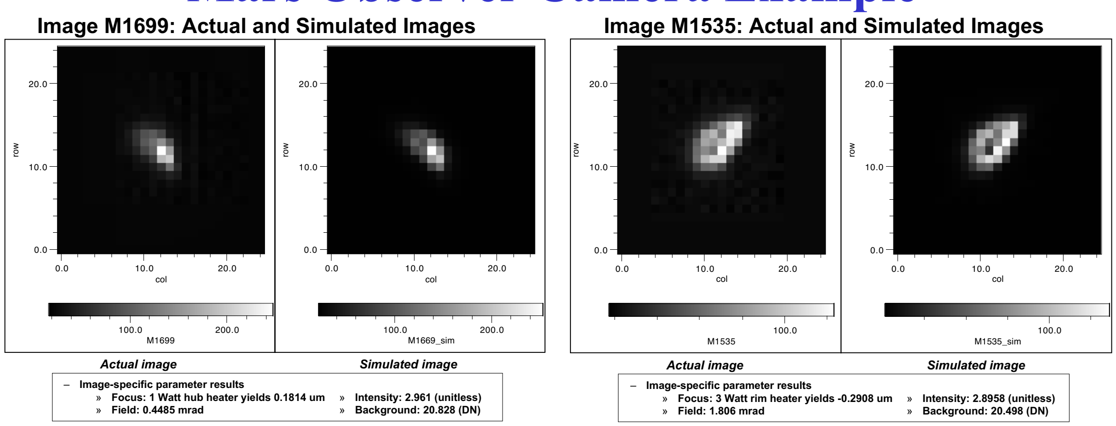

- Diagnostic data taken en route to Mars
- Illustrates prescription retrieval with relatively low resolution, low SNR data

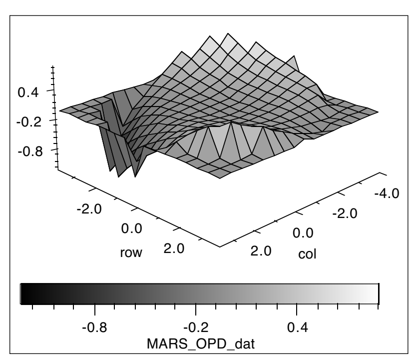

Image-Based WF Sensing Heritage Includes Hubble Space Telescope

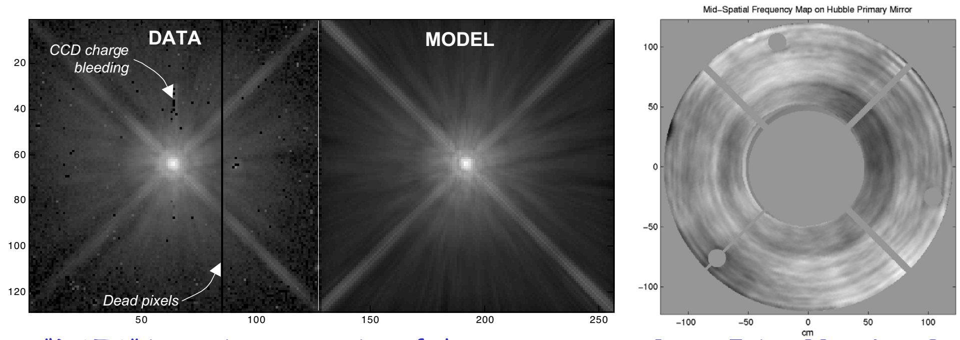

- "DATA" image is a composite of three exposures of star Feige 23, taken Oct 24, 1998 as a calibration image, displayed with a log10 stretch
  - Exposure times of 1, 4, 100 seconds provide high dynamic range
  - Taken with PC1 camera, F606W filter
- "MODEL" image is computed using HST model incorporating retrieved high-resolution mirror map
  - Map estimated using WF sensing operating on archival data
  - Model further optimized to match this image using prescription retrieval
  - Ref. J. Hutchings, D. Frenette, R. Hanisch, J. Mo, P. Dumont, D. Redding, S. Neff, "Imaging of z~2 QSO host galaxies with the HST," Astron. J., in press.

Phase Retrieval Camera (PRC)

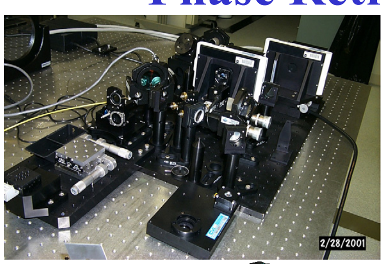

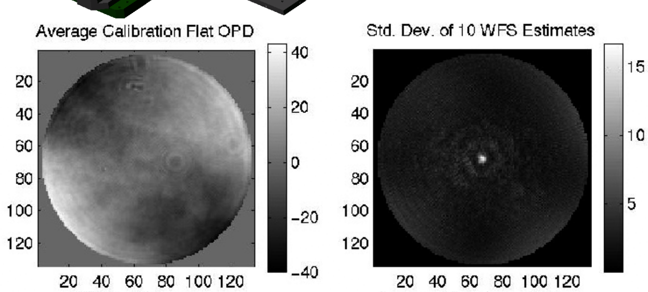

- An imaging camera for WF sensing
  - Provides a "portable WFC testbed" for use with NMSD, AMSD, other optics
  - Provides large optics WFC experience before NAR
- Calibrated performance (using internal calibration flat on flip stage)
  - 15.4 nm static WF aberration
  - 1/325 wave repeatability for low spatial frequency WF errors
  - Performance verified by comparison with Zygo interferometer

Cryogenic Deformable Mirror Technology

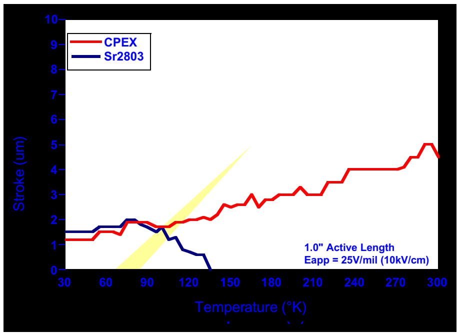

Cryoceramic materials for DM actuators meet stroke objectives over NGST operational temperature range

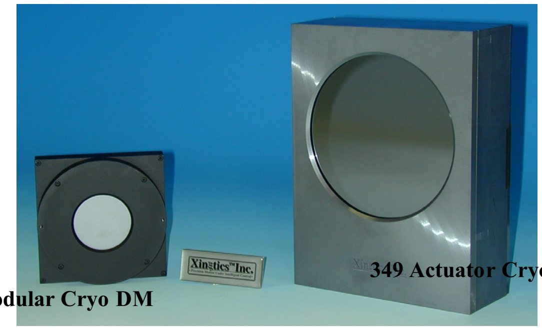

Modular Cryo DM

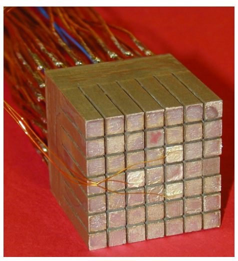

Modular actuator array with integrated electrical connections provides better performance, lower risk for cryo DM

- Deformable Mirror (DM) enables correction of primary mirror aberrations with a small optic elsewhere in the beam train
- Xinetics Inc. successfully developed Cryogenic DM technology and demonstrator mirrors meeting NGST requirements under a SBIR III
  - Developed an electrostrictive electroceramic for 35-65°K
  - Developed a piezoelectric electroceramic for 35-375°K
  - Completed 2 349-channel cryogenic DMs
  - Developed modular cryo DM technology and completed demonstrator DM
  - Successfully thermal cycled DMs to 35°K and demonstrated DM actuation at 50°K
- NGST contractors chose not to baseline a DM; however, technology is now available if actuated primary mirror does not meet performance requirements

Maintenance: PSF Monitoring and/or Metrology

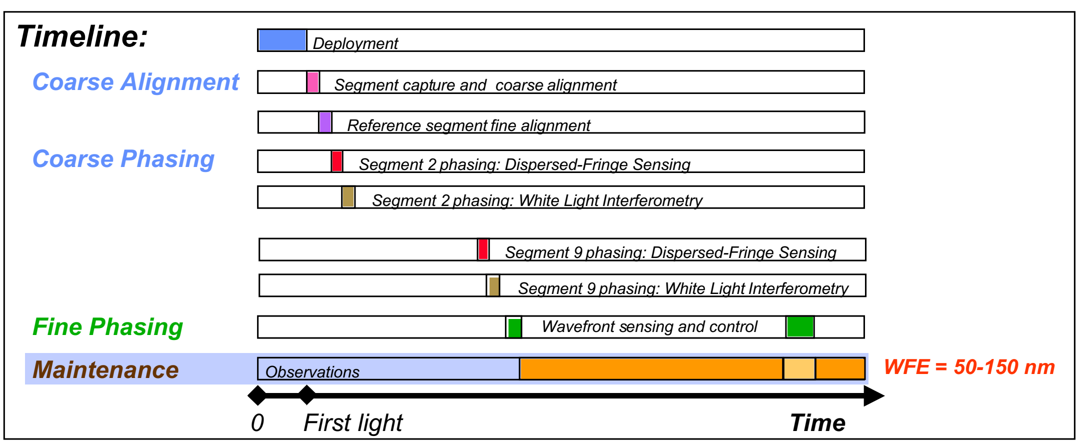

PSF Monitoring During Science

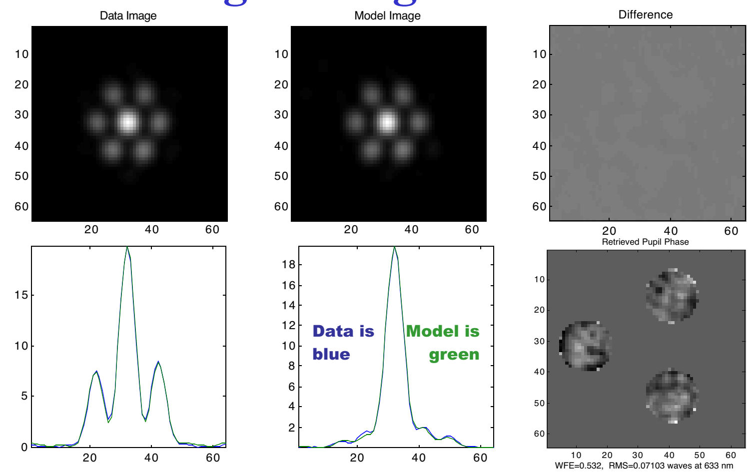

- "Infocus PSF Optimizer" (IPO) estimates WF from infocus imagery
- Experiments using WCT-2 show robust, accurate low spatial-frequency WF control
  - Measure and control tip-tilt-piston for 3 segments
  - Sensing range of λ/2 , accuracy of λ/100 demonstrated
- More complex 9- and 36-segment NGST apertures being studied in simulation

Piston Accuracy with PSF Magnifier (λ=900 nm)

Experiment (29 June 2001): **Simulation:**

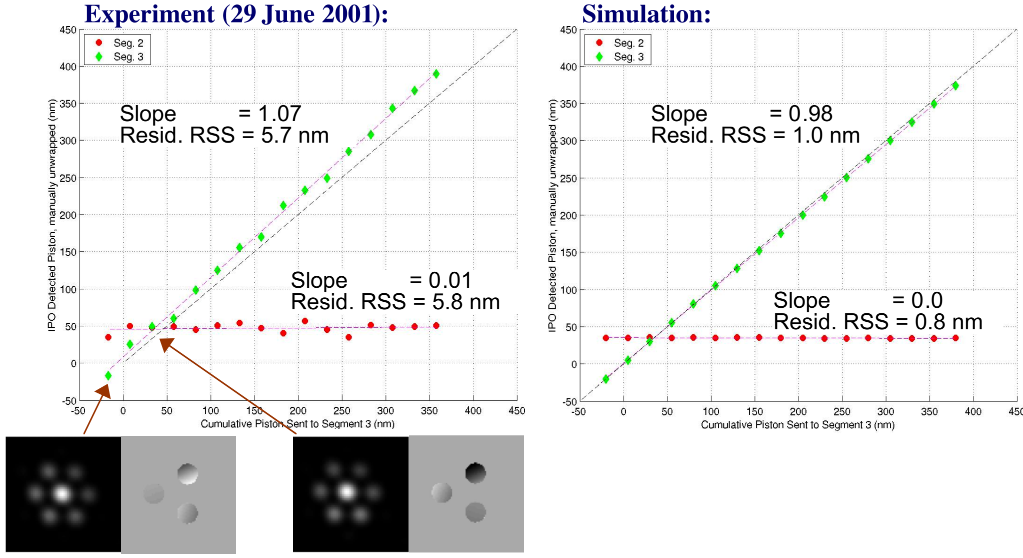

- Piston Seg. 3 in steps of +25 nm. Detected piston was manually unwrapped after 225 nm (λ/4).
- Residual errors show ~6 nm piston detection uncertainty (RSS), which is on the same order as the 5 nm PZT accuracy.

Control of Segmented PM using Metrology

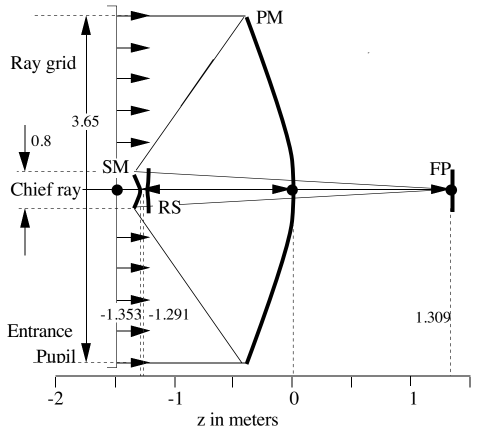

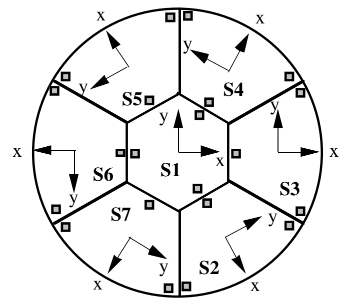

Does Sensor Configuration Observe Wavefront Errors?

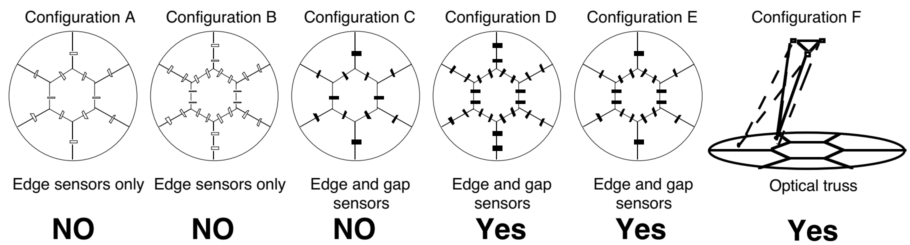

Laser Truss Application of SIM Metrology

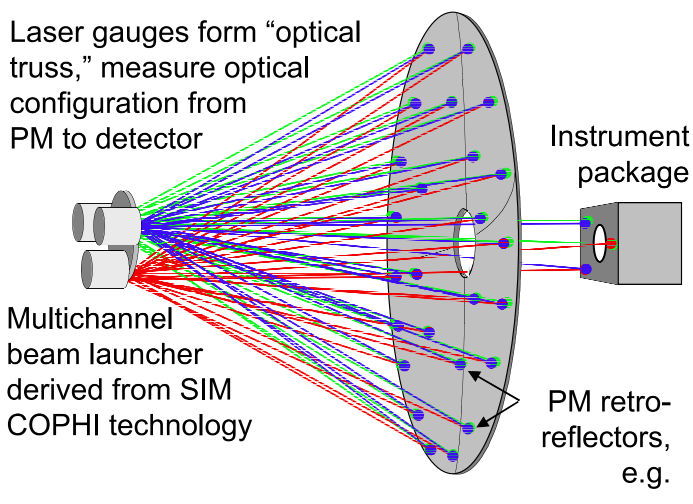

COPHI demonstrated performance in relative mode:

Sensing bandwidth	1Hz	100 Hz	10 kHz
Resolution	0.005 nm	0.02 nm	0.1 nm
Thermal Stability	Better than 1nm/K		

Laser truss can fully measure motions that affect optical quality

3 retroreflectors per segment for rigid-body motions, more for flex deformations

Absolute mode for large dynamic range, low accuracy

Relative mode for high accuracy

Optical fiber couples laser on warm side to cold beam launcher

Other configurations may be useful (backside of PM, for instance)

WFC Technology Heritage Matrix

Approximate Technology Readiness Levels (TRLs) for Cryo SubMM/FIR missions

Control Mode	NGST	PSR	SIM	SIRTF	Other
Capture	TRL4	TRL2			
Coarse Alignment	TRL4	TRL2			
Coarse Phasing					
White-Light Interferometry (WLI)	TRL4				TRL2?
Dispersed-Fringe Sensor (DFS)	TRL4				
Keck Phasing Camera					TRL2?
Fine Phasing					
Image-based WFS	TRL4			TRL6	
Dedicated WFS					TRL2?
Maintenance					
Edge sensing systems		TRL2			???
Laser truss metrology		TRL2	TRL4		
Cryogenic Components					
Segment actuators	TRL5				
DM actuators	TRL4				
Cryo edge/gap sensors		TRL2			???
DART membrane actuators					TRL2?

Conclusion

- NGST WFS&C system will be developed to TRL6 over the next few years
  - Tested in cryo-vac environment with traceable hardware
- SubMM problem is probably easier
  - Scales with wavelength
  - Likely to have a more stable environment
  - Detectors may present small complications
- New system approaches need a new look
  - DART membrane mirrors require a new actuation approach
  - Other mirror and actuation technologies may prove useful as well